e-Prime - Advances in Electrical Engineering, Electronics and Energy 8 (2024) 100564

Contents lists available at ScienceDirect

e-Prime - Advances in Electrical Engineering, Electronics and Energy

journal homepage: www.elsevier.com/locate/prime

Techno-economic optimization of a hybrid energy system with limited grid connection in pursuit of net zero carbon emissions for New Zealand

Daniel Hill [a], Shafiqur Rahman Tito [b], Michael Walmsley [b], John Hedengren [*,a]

[a] Department of Chemical Engineering, Brigham Young University, Provo, Utah, 84602, USA
[b] Ahuora Centre for Smart Energy Systems, University of Waikato, Hamilton, 3240, New Zealand

ARTICLE INFO

Original content: New Zealand Grid Optimization

Keywords:
Hybrid energy systems
Design optimization
Dispatch optimization
Optimization algorithms

ABSTRACT

As New Zealand moves towards net zero carbon emissions by 2050, multiple factors must be considered including increased electrical load due to electrification, variability of renewable energy generators, required storage capacity, system economics and limitations on grid transmission capacity. Complex and region-specific interactions between the various design choices involved are likely to require an understanding of a range of optimal and near-optimal designs for proposed micro-grid systems as opposed to a single optimal point. This work develops a novel multiscale optimization algorithm for optimization from a univariate capacity optimization approach to a multivariate one. This enhanced algorithm is applied to a grid-connected hybrid energy system consisting of local wind and solar generation, battery storage, and a limited grid connection for industrial and residential loads. This analysis is repeated for current 2023 and forecasted net zero 2050 grid conditions. Development of local generation allows for a 36.8% reduction of levelized cost of electricity in the 2023 case and a 38.6% reduction in the 2050 case. This results in a projected reduction of 19920 tonnes of CO_2/yr. The algorithm and methodology developed are broadly applicable to optimization of next-generation energy grids.

1. Introduction

There is an increasing motivation to reach net zero carbon emissions across the developed world. This includes reduced emissions from power generation, electrification of transportation, industry and residential energy demands. Existing generators producing carbon emissions can be replaced with renewable energy generation, yet the most broadly applicable renewable energy sources, wind and solar are non-dispatchable and intermittent. Storage and flexible loads can be critical tools to balance electricity generation and demand at all times as required for grid stability.

Under the Climate Change Response Act, New Zealand is committed to reaching net zero emissions of all non-biogenic greenhouse gases by 2050 [1]. Accomplishing this goal will require carefully-considered changes to building construction [2], transportation [3], economics, land use [4], power generation [5] and many other areas.

More specifically, managing net zero power generation in a cost-effective way will involve substantial changes to the New Zealand power grid and merits close analysis [6]. Analysis must include electrification of industrial [7], residential and transportation loads as well as tradeoffs between the various costs including grid infrastructure upgrades [8], buildout of additional carbon-neutral power generation and feedback response schemes [9].

Hybrid energy systems (HES) are proposed as a potential technology for reaching net zero emissions [10]. These systems integrate various forms of energy generation, storage and flexible loads to meet required energy demands in a reliable and cost-effective way [11]. HES have been studied for a wide range of systems including remote, grid-isolated systems [12], nuclear-integrated systems [13] and integration of alternative products such as hydrogen [14].

The New Zealand transmission grid, shown in Fig. 1, consists of several large population centers and many outlying smaller population centers connected by long transmission lines. Many of these outlying population centers have significant non-electrical energy loads that will need to be electrified in order for the country to reach net zero carbon emissions by 2050. These loads include non-electrical residential and industrial heating as well as transportation. The increased electrical load at terminal points on the power grid may exceed current transmission grid capacities for some locations, requiring expensive transmission grid upgrades.

Recent research has investigated localized, grid-connected smart microgrids as bottom-up energy generation schemes that can reduce

* Corresponding author.
E-mail address: john_hedengren@byu.edu (J. Hedengren).

https://doi.org/10.1016/j.prime.2024.100564
Received 11 October 2023; Received in revised form 6 February 2024; Accepted 26 April 2024
Available online 3 May 2024

transmission demand by balancing the local generation and demand to the extent possible [16,17]. This work aims to investigate the technoeconomic tradeoffs of optimal HES design when grid capacity expansion is a consideration in addition to local renewable energy generation and storage.

There are many optimization techniques and tools applicable to HES covering a broad array of potential requirements and assumptions. Broadly, these methods focus on either optimization of the design or operation of an HES or both. Each of these methods can be formulated as a minimization of an objective function (J) through use of well-known or novel numerical optimization techniques. The most prevalent techniques include gradient-based methods, gradient-free methods, and heuristic methods.

There are many variations of objective function formulations, but these functions generally include relevant capital and operating costs in addition other factors of interest such as system robustness, environmental impact, or special economic considerations. Objective function variables include a combination of design (x_{des}) variables, dispatch or operational (x_{op}) variables and other exogenous factors (x_{exog}) depending on the purpose of the optimization.

Both the design and operation can be optimized simultaneously by including both design and operational variables in a single objective function that is then minimized by direct application of well-known or novel numerical minimization techniques as shown in Eq. (1).

$$\underset{x_{des},x_{op}}{\text{minimize}} \quad J(x_{des}, x_{op}) \tag{1}$$

This method is referred in the remainder of this work as the direct solution to a combined design and dispatch optimization problem. While the direct solution is intuitive, this approach generally does not scale well to larger problems and quickly becomes intractable for complex systems being optimized over long time horizons.

For problems that are too complex or long to solve directly, a nested optimization method is often used. This method separates the design and

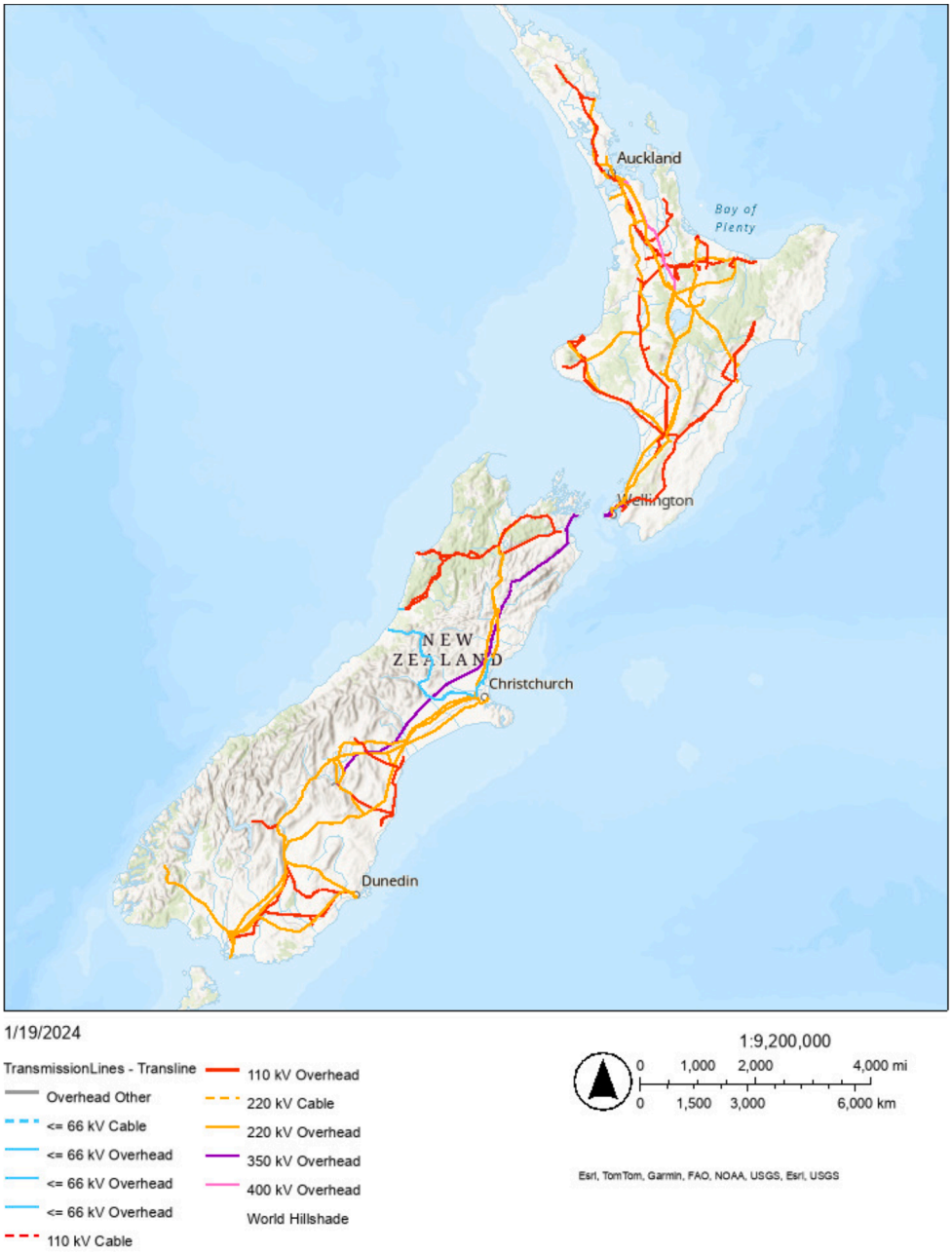

Fig. 1. Map of the New Zealand transmission grid including the ratings and types of each line [15].

dispatch optimization problems into nested layers where the outer layer optimizes the design, generally consisting of unit capacities, and the inner layer optimizes the dispatch or operation given a specific design. For each iteration of the outer loop the system design is fixed, the operation for the given fixed design is optimized using the inner layer, and the outer objective function value is calculated. This process is repeated with further iterations of the outer layer until the optimization converges to both an optimal design and dispatch for the design. This strategy is represented mathematically in Eq. (2) where J is used to represent an outer design optimization problem and K represents an inner dispatch optimization.

$$\underset{x_{des}}{\text{minimize}} \quad J(x_{des}, x_{op}) \tag{2a}$$

$$\text{subject to :} \tag{2b}$$

$$x_{op} = \text{argmin} K(x_{op}) \tag{2c}$$

Many software packages implementing variations of direct and nested optimization are readily available through free and commercial sources. The RAVEN/HERON toolset uses a nested approach most often combined with stochastic or other gradient-descent techniques [18]. Other widely-used tools using variations of these methods include REopt [19], iHOGA/MHOGA [20] and HOMER [21]. A deeper comparison of various techniques and available software packages for HES optimization is given by Sinha and Chandel [22] as well as in the introduction to recent work by Tukee et al. [23].

There are a number of limitations with current combined design and dispatch optimization methods. Many of these methods, particularly the direct approach, do not scale well and tend to quickly become intractable as problems become more complex and are optimized over longer time horizons [24]. This frequently results in additional model approximations (e.g. linearization) and simplifications (e.g. shorter time horizons) in order to improve the tractability of the problem. Such approximations and simplifications limit the accuracy of the resulting solution.

In addition, most currently implemented methods do not implement any sensitivity analysis as part of the algorithm, resulting in a lack of understanding of the results in perturbations surrounding the optimal point. While optimization methods and feasibility analysis methods can be combined, this leads to additional complexity and determining an efficient sampling of the input space for these methods can be challenging [25].

This work develops a novel, multiscale, combined design and dispatch optimization method that addresses both of these challenges. While a previous implementation [24] has been proven to provide detailed technoeconomic tradeoff information in addition to solving long time horizons, the method was effectively limited to a univariate analysis for the design optimization. This work builds on the previous work by expanding this analysis to fully multivariate design optimization cases while demonstrating application to a challenging and unique HES optimization. This method is anticipated to be useful for those analyzing and designing hybrid energy systems requiring complex and detailed optimization, particularly in cases where detailed technoeconomic tradeoff information is desirable.

2. Methodology

Analysis for this work is based on a simple grid-connected hybrid energy system that represents a generic, terminal portion of the New Zealand power grid. This HES is first modeled to approximate current (2023) grid conditions and is then expanded to include anticipated growth and electrical load changes between 2023 and 2050. These changes include efforts to transition to net zero carbon emissions throughout industrial, residential and infrastructure domains.

For both the 2023 and 2050 cases, the various generation capacities are optimized using a unique multiscale techno-economic optimization technique to determine the optimal power generation, storage and grid interconnection capacities. This work considers dispatch on an hourly basis. There are expected to be significant sub-hour changes with an increase in local wind and solar generation that would need to be handled in some way, most likely using electrical batteries. This sub-hour variability lies outside the scope of this work.

2.1. Hybrid energy system model

The base HES system consists of wind and solar generation as well as industrial and residential loads, an electrical battery and a grid exit point. For the 2050 case electrical vehicle charging is also included as an additional load. This HES is intended to represent the state of parts of the New Zealand power grid, although it does not represent any one particular location and parts of the system are based on data from across the country.

The residential load in this work is modeled as a fixed time series that approximates the load used by 1000 typical homes in New Zealand. The industrial load is based off real data obtained from an anonymous meat processing facility as discussed in Section 3. Both residential and industrial loads are treated as fixed loads with no demand-side response. The load from electrical vehicle charging, where applicable, is set as a fixed time series representing likely charging patterns considering existing demand-side response mechanisms.

Local generation consists of wind and solar sources combined with electrical battery energy storage. Both wind and solar generation data are obtained from NIWA and are scaled according to the respective installed capacities. Any electrical imbalance between the local generation and load is met by the connection to the larger power grid, the local electrical battery or both. A diagram of the various components and interconnection of the system are shown in Fig. 2.

The carbon emissions of the HES are approximated based on per capita carbon emissions for New Zealand (6.2 tonnes/person [26]), the number of households in the HES and the average number of people in a New Zealand household (2.7 [27]). This results in a total of 16740 tonnes of CO_2/yr for the 2023 case and 19920.6 tonnes of CO_2/yr for the 2050 case.

The installed wind and solar capacity as well as the battery capacity and grid interconnection limit are optimized for minimization of the levelized cost of electricity (LCOE) while meeting the system demand. The optimization problem for the HES is described mathematically in Equation 3.

$$\underset{x_{design}, x_{dispatch}}{\text{minimize}} \quad LCOE \tag{3a}$$

$$\text{subject to} \quad LCOE = \frac{\sum_{n=0}^{n_{comp}} (C_n) + C_{grid}}{\sum_{t=0}^{m_{hrs}} \left(E_{resid,t} + E_{indus,t}\right)} \tag{3b}$$

$$C_n = C_{Cap,n} N_n \frac{L_{sys}}{L_n} + C_{FOC,n} L_{sys} + C_{VOC,n} \sum_{t=0}^{m_{hrs}} E_{n,t} \quad \forall \quad n \in [\text{wind}, \text{solar}, \text{battery}] \tag{3c}$$

$$C_{grid} = C_{cap,grid} + E_{import} C_{import} - E_{export} C_{export} \tag{3d}$$

$$C_{cap,grid} = a \arctan\left(N_{grid} + b\right) + c + d\left(N_{grid} - 4\right) \tag{3e}$$

$$0 = E_{wind} + E_{solar} + E_{battery} - E_{resid} - E_{indus} + E_{import} - E_{export} - E_{curtail} \tag{3f}$$

$$0 \le E_n \le N_{grid} \quad \forall \quad n \in [\text{import}, \text{export}] \tag{3g}$$

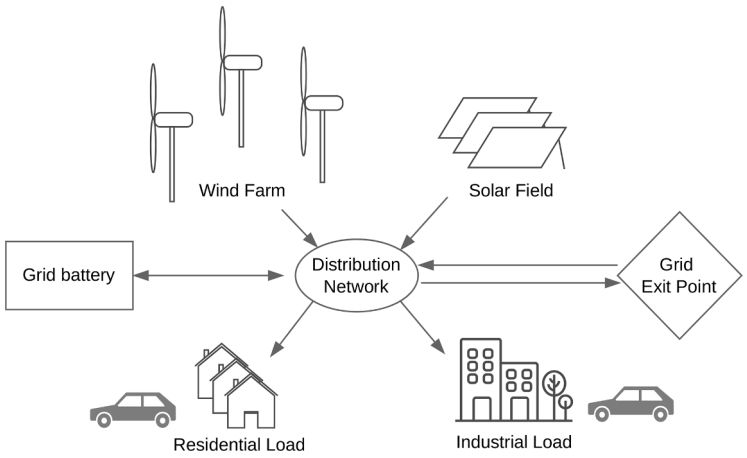

Fig. 2. Layout of the grid-connected hybrid energy system. Arrows represent the flow of electricity.

$$N_{n,\min} \leq N_n \leq N_{n,\max} \qquad \forall \quad n \in [\text{wind}, \text{solar}, \text{grid}, \text{battery}] \tag{3h}$$

$$B_{SOC,t} = \int_0^t E_{battery} \qquad \forall \quad t \in n_{hrs} \tag{3i}$$

$$0 \leq B_{SOC} \leq N_{battery} \tag{3j}$$

$$E_{curtail} \geq 0 \tag{3k}$$

The overall objective (Eq. (3a)) is to minimize the system LCOE while meeting the required constraints (Eqs. (3b)-(3k)). The optimization variables consist of design variables (x_{design}) and system dispatch variables ($x_{dispatch}$). The design variables are the installed wind (N_{wind}), solar (N_{solar}), grid interconnection limit (N_{grid}) and battery ($N_{battery}$) capacities. The dispatch variables are the electricity bought from (E_{import}) and sold back (E_{export}) to the grid, the energy stored or retrieved from the electrical battery ($E_{battery}$) and the energy lost due to curtailment of renewable generation ($E_{curtail}$). This combination of design and dispatch variables highlights the tradeoff between various design capacities and system dispatch that is often found in grid optimization problems.

The LCOE (Eq. (3b)) is calculated as the sum of costs divided by the total amount of power provided. The costs include the capital, fixed and variable operating costs for the wind and solar generators and battery (3h), as well as the net cost of electricity exchange with the grid (Eq. (3d)). For simplicity, the time value of money is not considered in this work. The net cost of the grid consists of capital costs required to expand the grid interconnection capacity beyond the current rating (Eq. (3e)) and the net cost of electricity bought and sold to the grid through the grid exit point. The economics presented here are for demonstration and are not intended to represent any particular real system.

There are significant non-electrical energy loads in this base system. Approximately 89% of the energy required for the meat factory each year is currently met by onsite coal boilers. Transportation in this base case consists largely of fossil fuel vehicles. Both of these are significant emissions sources and anticipated to be phased out by 2050. Any other non-electrical energy loads in the system are not addressed in this work. The impact of importing and exporting power to the grid on the electricity prices is not considered. Other details not described here are neglected in this work including solar panel degradation over time and battery round trip efficiency.

Two specific cases of this model are considered in this work for insight into future grid design. The first case is meant to represent current grid conditions in New Zealand. The second is intended to represent a net zero carbon emissions power grid in 2050. Both cases use the mathematical model described in Eq. (3), but with different parameters and time series to represent the aspects unique to each circumstance. Numerical values for the differing model parameters can be found in Section 3.1. Additional details about the involved time series can be found in Section 3. Perturbation in renewables generation is not explicitly modeled or accounted for in the model or optimization, but are inherently covered to some extent due to the variations captured over the length of the time series.

2.2. Forecasted grid changes

Many aspects of the current power grid are expected to change between now and reaching net zero carbon emissions in 2050. While many of the changes are difficult to predict, some basic anticipated changes to the grid are accounted for in this work and are described below. Anticipated changes not considered in this work include changes in electricity prices, changes in electricity usage patterns and increased demand-side response.

2.2.1. Increased residential load

The residential electrical load is expected to increase across New Zealand due to continued population growth, electrification of residential appliances and increased standard of living. Additional considerations include increased appliance and home energy efficiency, Jevons Paradox, and an anticipated increase in residential solar and home battery installations. Finally, increased adoption of electric vehicles will also likely change the dynamics and magnitude of residential loads.

Predicting the exact dynamics and magnitude of a representative residential load for New Zealand for 2050 is outside the scope of this work, but the following assumptions are used to make a usable prediction for this work based on the base 2023 residential load profile.

1. The residential electrical load is increased by 19% at each time point to account for a corresponding increase in population as anticipated by NZ.Stat [28]. This population increase creates a corresponding increase in the expected carbon emissions to 19920.6 tonnes/yr for the 2050 case.
2. One third of the electric vehicles are charged at home during the night. This is assumed to be controlled by some form of demand response such that the charging load is spread evenly across the low price hours (10 PM-7 AM). More detail is presented in the section on electric vehicles (Section 2.2.3).
3. The houses have on average an additional 5 square meters of residential solar added between 2023 and 2050 for a total of 1.12 MW installed capacity. This generation follows the same dynamics as the industrial solar generation.
4. The houses have on average a 5 kWh home electrical battery added. This equates to a total electrical battery storage capacity of 5.6 MWh.

2.2.2. Electrification of industrial load

A critical aspect of reaching net zero carbon emissions in New Zealand will be the electrification of industrial energy requirements. The industrial load used in this work is a meat processing facility studied recently by Klinac et al. [29].

This meat factory processes over 2 million animals a year and exports to over 80 countries providing a significant part of the local economy. The site includes slaughter, boning, casings, rendering and fellmongery facilities. The products include meat cuts, offal, lamb skins, wool, bood meal, bone meal and tallow. Current electrical loads for the site include refrigeration, multiple electrode boilers, and various types of heavy equipment. This electrical load comes to a total of 9.7 GWh over the course of a full year.

In addition to the electrical load, there are two coal boilers currently providing 79.3 GWh_{th} per year. This study assumes that these two coal boilers are replaced with two high temperature heat pumps and one ultra-high temperature heat pump, which combined provide the same required thermal load. This electrification of thermal loads increases the average electrical load value by 433%. The rate of change in the load in this scenario also increases significantly.

Fig. 3 captures the dynamics of both the current and net zero 2050 case electrical loads. While there is some current thermal storage of hot water throughout the site, additional thermal storage would likely be installed to smooth the required electrical load [30]. The impact of additional thermal storage for the site lies outside the scope of this work.

2.2.3. Electric or hydrogen-based vehicles

A transition away from fossil fuel vehicles will be an essential part of reaching net zero carbon emissions. For this work, vehicles are anticipated to have transitioned to electric by 2050. This increase in electric vehicles has significant impact on the local power grid through the increased need for charging.

It is assumed that there are 1200 vehicles (approximately one per house) needing charging for 40 km each day. Of these, 800 vehicles are charged at home and result in an increased residential load. The vehicles are assumed to be charged at home during the lowest cost periods of each day (10PM-7AM) in such a way that the entire load is evenly spread between these hours. This imitates the ripple control currently used for residential water heaters in New Zealand [31]. It is assumed to require 0.180 kWh/km for charging [32]. This results in an additional 5.76 MWh at a charging rate of 0.640 MWh per hour.

Another 400 vehicles are assumed to be charged at car parks during normal working hours (9AM-4PM), which is another low-cost period of day. This non-residential load is added to the industrial load to represent the idea that car charging parks are likely to exist in commercial and industrial locations.

Electric vehicle charging is estimated this way as an approximate demand-side response. A large fraction of water heaters in New Zealand are on ripple control, so this extension to electric vehicles seems reasonable.

There is significant uncertainty in how decarbonization of heavy trucking will be done in New Zealand with two main options being hydrogen-powered and electric trucking. The impacts of this decarbonization, while important for the environment, are not anticipated to have a heavy impact this analysis and are not considered in this work.

2.2.4. Potential grid transmission line upgrades

Portions of the New Zealand power grid are likely to need upgrading in order to handle increased electricity transmission. Grid transmission upgrades are anticipated in this work to be very expensive per megawatt capacity for any initial upgrade, but decrease to a lower per megawatt cost for large capacity upgrades. This is assumed as any upgrade will likely require initially staffing of the project, rebuilding transmission towers and replacing existing transformers, transmission wire and switchgear. Once replacement of the infrastructure is already accounted for, replacing with higher-capacity components is anticipated to be comparatively smaller in cost.

The capital cost associated with a particular grid capacity is mathematically modeled in Eq. (4) and plotted in Fig. 4 where the high and low per megawatt cost regions are labeled Region 1 and Region 2 respectively. Eq. (4) is continuous in the first derivative, facilitating efficient optimization. The parameters for the equation are given in Table 1.

$$C_{cap,grid} = a\arctan\left(N_{grid} + b\right) + c + d\left(N_{grid} - N_{grid,\min}\right) \tag{4}$$

Note that Eq. (4) was developed for this work as a best estimate for transmission line costing in the absence of better information. The real cost of transmission line upgrades is expected to be heavily situation dependent. The transmission distance, terrain type, required voltage and many other factors heavily impact the capital cost. Transmission lines could also be broken into multiple sections with differing requirements and sections needing upgrade at different transmission limits. Detailed costing of transmission line upgrades lies outside the scope of this work yet Eq. (4) is meant to serve as a sample cost function that exposes useful insights into relevant technoeconomics that may be encountered in real systems.

For this work, the length of the transmission line requiring upgrade is assumed to be 150 km, which is approximately the distance between Nelson and Westport. For reference, a technical report on pricing of several transmission lines in Australia [33] estimates transmission line capital costs at 0.6-1 million AUD/km. At a rate of 0.8 million NZD/km, a 150 km line would cost about 120 million NZD.

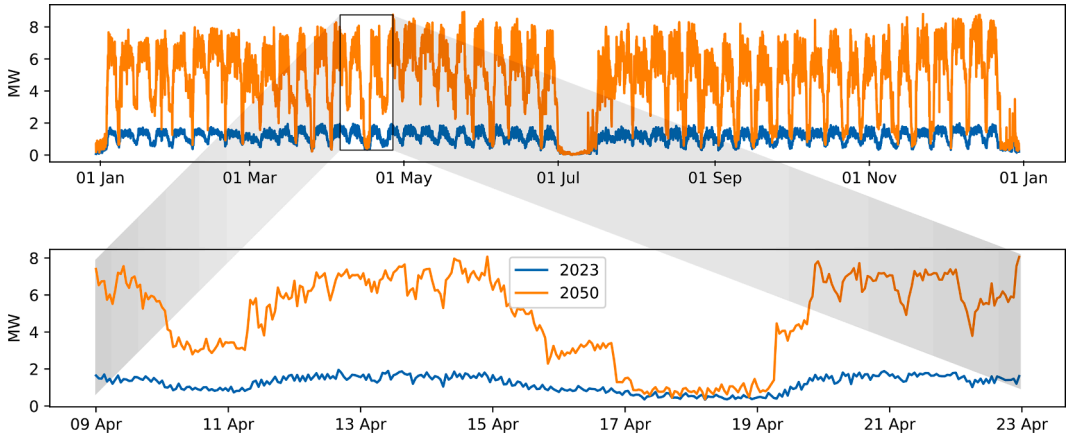

Fig. 3. Full-year and two-week sample of the industrial electrical load before (2023) and after (2050) electrification.

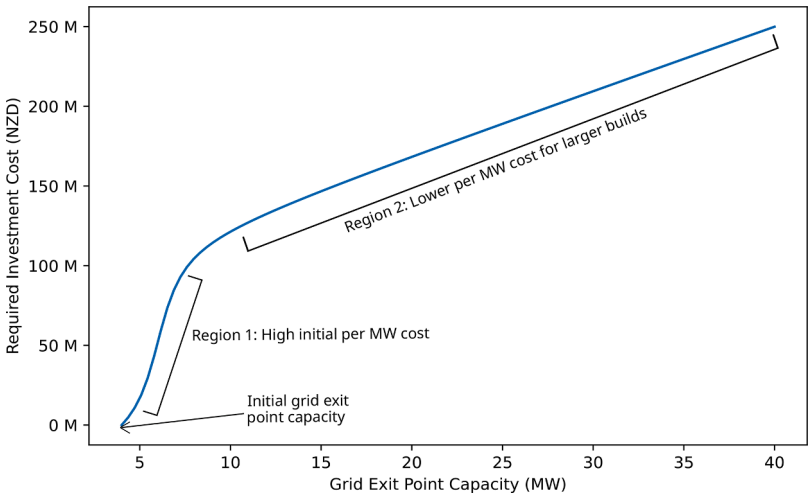

Fig. 4. The cost curve used for estimating grid transmission infrastructure upgrades.

Table 1
Parameters for transmission capital costing.

Parameter	Value	Units
a	40e6	NZD/MW
b	-6	MW
c	44285949	NZD
d	4e6	NZD/MW

2.3. Optimization technique

Optimization problems described in this work are solved using the GEKKO Optimization Suite [34]. GEKKO is a well-known and powerful solution for modeling and optimizing dynamic processes through a flexible modeling language. This optimization platform leverages large-scale solvers such as IPOPT to support LP, QP, NLP, MILP, and MINLP programming and has been applied to a broad range of fields including cogeneration, enhanced oil recovery, polyethylene reactors and many other complex processes.

A GEKKO [34] implementation of the mathematical model described in Eq. (3) over a full year results in a nonlinear optimization problem with 166452 variables and 148903 constraints. A single calculated optimal design, while useful, does little to outline the technoeconomic tradeoffs associated with this problem. To address this weakness, a previously-developed technique for multiscale optimization of hybrid energy system design and dispatch is applied [24].

This method consists of two stages: approximating a multi-dimensional distribution of the optimal capacities and evaluating the performance metrics at various samples from the distribution. The result is not a single optimal design, but rather performance metrics for a multi-dimensional range of capacities that are likely to be optimal or near-optimal.

This algorithm starts with computing the exact solution for the real problem, but over a short subset (length τ) of the full time period. This is repeated for many different subsets of the full time period. Each of these smaller problems will have optimal capacities which are then combined into a multi-dimensional distribution of optimal capacities for the system. Additional details on this step are available in the cited previous work.

The second stage of this method consists of sampling unit capacities from the optimal capacity distribution and evaluating various performance metrics for the system when the sampled capacities are used for the full time period. Details on the metrics evaluated are given in Section 2.4. In contrast with the initial implementation of the this method, the samples are randomly selected directly from the multi-dimensional optimal capacity distribution rather than assembled from univariate distributions for each of the capacities being optimized.

The results of this method are represented in two ways in this work. The first is a pairplot of the multi-dimensional optimal capacity distribution, providing insight into the various combinations of capacities that are likely to be optimal or near-optimal. In these pairplots, each scatter plot represents a two-dimensional view of the multi-dimensional optimal capacity distribution with the associated axis indicating which dimensions are considered. The plots along the diagonal of the figure are histograms on a single dimension of the distribution, allowing another perspective of the data.

The second representation of the results consists of scatter plots of the various metrics against relevant design capacities, providing insight into how the various metrics vary as a function of the design capacities. Additional detail about the distribution dimensions considered are given with each figure. Where possible, the traditional solution to the full optimization problem is also computed and overlaid in the result plots for validation and comparison.

All of the optimization problems described in this work were solved using GEKKO 1.0.6 [34] and IPOPT 3.12.10 [35] on an AMD Ryzen 7 2700 processor with 16 Gb RAM and a 1 Tb M.2 SSD drive. A subset length (τ) of 240 h was used for all calculations.

2.4. Metrics

Various metrics are used to analyze the performance of each combination of unit capacities considered in this work. These metrics are intended to provide insight into the relative performance of various possible system configurations.

1. The Levelized Cost of Electricity (LCOE) is used to measure the economics of the system. This measure consists of the total perceived costs for electricity production normalized by the amount of electricity provided as shown in Eq. (3b).
2. The percent local generation describes the fraction of locally required power that is produced locally. This is a measure of reliance on the larger New Zealand electrical grid.
3. The total curtailment for the system represents the total amount of electrical power produced by renewable energy generators that is curtailed to prevent oversupply of electricity.

3. Data sources

The wind and solar time series data is based on profiles generated from the NIWA SolarView calculator for representative locations in New

Zealand [36]. The wind and solar irradiance profiles were then converted to the corresponding amount of generated electrical energy using the same methods described in recent work by Tito et al. [37]. These time series result in a solar capacity factor of 13.8% and a wind capacity factor of 18.2% over the full year of data. The residential load for this system (E_{resid}) is based of a weighted average of 24 typical New Zealand homes as used in recent work by Apperley and Toki [16] and scaled up to 1000 homes for the 2023 case. These time series data sources are intended to be representative of a single year of operational data and include intermittency in both renewables generation and system loads.

The meat factory electrical load before and after electrification is obtained from recent work by Walmsley et al. [38]. This data includes characteristic shutdown times for the plant for cleaning and maintenance twice a year.

The grid purchase price (C_{import}) is estimated based on a tiered pricing consisting of peak, medium and low demand times. The peak price is 0.3 NZD/kWh and covers 7–9 AM and 4–8 PM each day. The medium price is 0.18 NZD/kWh and covers 9 AM-4 PM and 8 PM-10 PM each day. The low price is 0.1 NZD/kWh and covers from 10 PM-7 AM. This is based on estimations from those familiar with New Zealand electricity pricing. A "line charge" of 0.11 NZD/kWh is then added uniformly to the bulk electricity prices to represent the line charges used to maintain the grid infrastructure. These prices are based on personal knowledge of current New Zealand electrical prices. The electricity buyback price (C_{export}) is estimated at 0.07 NZD/kWh. This is estimated based on sources that estimate the residential buyback price at 0.07-0.17 NZD/kWh [39].

3.1. System parameters

Parameters for the model in Equation 3 cover both technical and economic aspects of the system. The technical parameters, shown in Table 2, including the anticipated lifetimes as well as lower and upper capacity bounds for each of the components. These parameters are used for both the 2023 and 2050 cases.

The economic parameters cover the capital, fixed and variable operating costs for the solar, wind and electrical battery components. These parameters are expected to change over time with the 2023 and 2050 parameters shown in Tables 3 and 4.

There is significant uncertainty around many of the system parameters. Some of the parameters vary geographically, vary in time, are not publicly available or are heavily dependent on other factors like the system design. This uncertainty increases significantly when projecting to the year 2050. A comprehensive review of the parameter projections to 2050 is not only outside the scope of this work, but also necessarily makes many assumptions about future grid conditions, consumer habits and technological advancements that are unknown. Parameters in this section are given merely as best guess estimates founded on data where possible. Sources are indicated next to each table value that is retrieved or estimated from literature. Previous work demonstrates a methodology for quantifying the uncertainty for similar parameters in a similar model [44]. Overall, the focus of this work is not a close analysis of a particular real system, but of a representative system from which important understanding of techno-economic tradeoffs can be drawn.

Table 2
Technical model parameters.

Symbol	Value	Description
L_{solar}	20 years [40]	Useful life of solar panels
L_{wind}	20 years [40]	Useful life of wind turbines
$L_{battery}$	15 years [41]	Useful life of the electrical battery
L_{grid}	60 years	Useful life of transmission line upgrades
L_{system}	30 years	Useful life of the system
$N_{solar,\min}$	0 MW	Minimum solar capacity
$N_{solar,\max}$	200 MW	Maximum solar capacity
$N_{wind,\min}$	0 MW	Minimum wind capacity
$N_{wind,\max}$	200 MW	Maximum wind capacity
$N_{grid,\min}$	4 MW	Minimum (current) grid transmission capacity
$N_{grid,\max}$	200 MW	Maximum grid transmission capacity
$N_{battery,\min}$	0 MWh	Minimum battery capacity
$N_{battery,\max}$	400 MWh	Maximum battery capacity

Table 3
Economic model parameters for the 2023 case.

Symbol	Value	Description
$C_{cap,solar}$	1980 NZD/kW [40]	Capital cost for building solar
$C_{cap,wind}$	2570 NZD/kW [42]	Capital cost for building wind
$C_{cap,battery}$	578 NZD/kWh [41]	Capital cost for building the battery
$C_{FOC,solar}$	0.00 NZD/kW [42]	Fixed operating cost for solar
$C_{FOC,wind}$	0.00 NZD/kW [42]	Fixed operating cost for wind
$C_{FOC,battery}$	24.8 NZD/kWh [41]	Fixed operating cost for the battery
$C_{VOC,solar}$	16.5 NZD/MWh [42]	Variable operating cost for solar
$C_{VOC,wind}$	16.5 NZD/MWh [42]	Variable operating cost for wind
$C_{VOC,battery}$	0.00 NZD/kW [41]	Variable operating cost for the battery

Table 4
Economic model parameters for the 2050 case.

Symbol	Value	Description
$C_{cap,solar}$	1160 NZD/kW [43]	Capital cost for building solar
$C_{cap,wind}$	2380 NZD/kW [42]	Capital cost for building wind
$C_{cap,battery}$	248 NZD/kWh [41]	Capital cost for building the battery
$C_{FOC,solar}$	0.00 NZD/kW [42]	Fixed operating cost for solar
$C_{FOC,wind}$	0.00 NZD/kW [42]	Fixed operating cost for wind
$C_{FOC,battery}$	24.8 NZD/kWh [41]	Fixed operating cost for the battery
$C_{VOC,solar}$	16.5 NZD/MWh [42]	Variable operating cost for solar
$C_{VOC,wind}$	16.5 NZD/MWh [42]	Variable operating cost for wind
$C_{VOC,battery}$	0.00 NZD/kW [41]	Variable operating cost for the battery

4. Results

Optimization of both cases provides insight into the complex tradeoff between economics and technical limitations involved in this problem. While the exact parameters likely do not apply to any particular real system, the technique used for optimization and analysis is generally applicable and there are multiple insights that are likely applicable to similar real systems that will be making changes in the near future to reach net zero carbon emissions.

As a benchmark for comparison, the LCOE for the 2023 case is 295 NZD/MW when no local generation or storage is built. For the 2050 case the LCOE is 316 NZD/MW for a system with an expanded grid capacity of 20 MW and no local generation or storage. These values represent the status quo or "business as usual" economics of the system.

4.1. 2023 Base case

A pairplot of the optimal capacity distribution for the 2023 case is shown in Fig. 5 and the exact solution to the problem overlaid using a gold star in each subplot. The exact solution lies within the region defined by the optimal capacity distribution indicating agreement between the two methods. The maximum load for the 2023 case is less than the base grid interconnect capacity (4 MW). As anticipated, a grid interconnect upgrade is not optimal as determined by either algorithm, yet building at least some local wind and solar generation as well as battery storage is anticipated to reduce the system LCOE from a reference of 295 NZD/MW to between roughly 100 and 250 NZD/MW.

A total of 1000 samples were taken and the proposed metrics were evaluated for each. These results are summarized in Fig. 6 and provide insight into how the various metrics change with changes in system design. The transmission capacity is not plotted as all cases used the base transmission capacity of 4 MW. The gold star in Fig. 6 indicates the exact solution when curtailment is allowed. There is once again agreement between the two analysis methods used. For reference, the red star

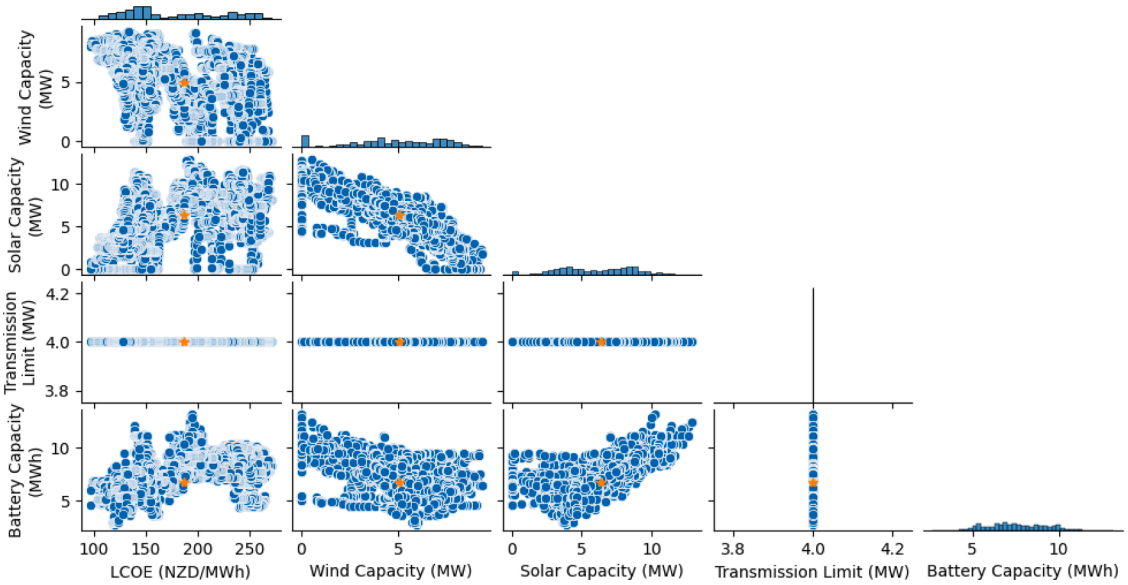

Fig. 5. Optimization Results for the 2023 case using curtailment. Gold stars mark the exact solution to the problem.

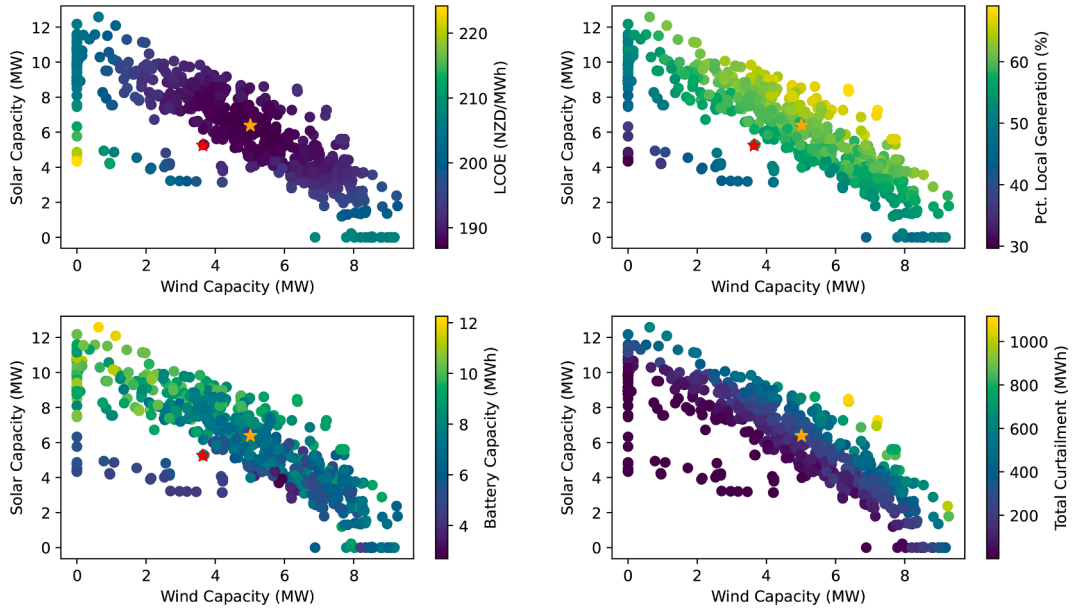

Fig. 6. Key metrics for the 2023 base case. Gold stars indicate the metrics at the exact solution with curtailment and red stars indicate the metrics at the exact solution without curtailment.

indicates the exact solution when curtailment is disallowed in all but the curtailment subplots.

Allowing for curtailment of the locally-generated renewable electricity increases the optimal local renewable generation capacities. It also increases the fraction of electricity generated locally from 56.0% to 60.8% and decreases the LCOE from 190 NZD/MW to 186 NZD/MW. Allowing for curtailment can also improve system reliability by allowing for a larger range of operations for the HES without increasing the likelihood of and unavoidable mismatch between supply and demand. Building more renewable generation capacities that periodically exceed the local load and export capacity can be economically and technically favorable. Integration of local demand response to local generation similar to the "ripple control" currently used for water heaters could reduce necessary curtailment in a real system.

The LCOE at the optimum unit capacities does not vary significantly for similar capacity designs. While it cannot be assumed that all or the majority of grid-connected HES will have similarly flat objective function values near the optimum, but this is clearly the case for some HES. The additional context provided by the multiscale analysis could be highly relevant when additional technical or economic details must be considered that are not included in the HES model.

A combination of wind and solar also appears to be techo-economically preferable as compared to building out just wind or solar capacities, although the exact ratio of the capacities does not appear to be critical to performance. A combination of renewable energy sources also yields the highest amount of locally generated power, improving the HES system independence. The optimal battery capacity is quite variable, but is more correlated with the local solar capacity than it is for local wind capacity.

4.2. 2050 Net zero case

A pairplot of the 2050 net zero carbon emissions case is shown in Fig. 7 with the direct solution to Eq. (3a) shown using gold stars in each subplot. There is good agreement between the two methods and a similar predicted reduction of LCOE as in the 2023 case. Less than 1 percent of the sampled time windows had extreme values for the transmission capacity ($\geq$ 100 MW). These values are excluded from the pairplot for clarity. Exporting large amounts of power, as the extreme values indicate, would likely impact the price of electricity across the grid, which is outside the scope of this work.

The ranges of optimal capacities for the 2050 case are an order of magnitude larger than the capacities for the 2023 case. The maximum local electrical load (11.08 MW) exceeds the base grid exit point capacity (4 MW), yet the transmission capacity increase appears to only be needed for a small fraction of the year as indicated by the histogram of transmission capacities showing a very large number of sampled time windows where the optimal transmission capacity remaining at the base value.

The metrics for 1000 sampled points from the optimal capacity distribution are shown in Fig. 8 with the metrics for the direct solution to Eq. (3a) shown using a white star. The sampled points that resulted in an HES unable to meet the local load over the full time series are shown in red. For clarity, the wind and solar generation capacities have been summed into the total renewable generation capacity.

While the optimal capacity distribution shows a large amount of values with no grid capacity expansion, none of these prove to be feasible when the dynamics of a full year are considered. Additionally, the exact solution does not require much grid expansion, but the surrounding points all have infeasibilities. This demonstrates how a knowledge of the technoeconomic tradeoffs surrounding an optimal design are essential for proper HES design. Building at the solution to the exact problem would likely give the lowest LCOE if the times series used were perfect predictions, but an HES with these fixed capacities would likely not be robust to variations in the time series or other system parameters. The LCOE of the system as shown in Fig. 8, is relatively constant near the optimum capacities, allowing for selection of capacities that improve system reliability without significantly increasing the LCOE.

From another perspective, these results indicate that the system does not require grid expansion for much of the year, but does require additional grid capacity for a small portion of the year. Additional effort could be applied to identify ways to reduce local load or increase local generation at the few high-load periods of the year, thus allowing for significant cost reduction to the system. These efforts could include additional demand-side response, adjusting factory scheduling, periodic usage of electric vehicles as grid batteries, or the building of a small amount of local peaking generation. Once again, this highlights the techno-economic impacts of investigating additional solutions near the exact optimum.

Adding curtailment for the 2050 case decreases the LCOE of the direct solution from 206 NZD/MWh to 194 NZD/MWh. Once again, this increases the local generation capacities, which also allows reducing the grid transmission capacity. Allowing for curtailment in the system also increases the percent of locally-generated electricity from 64.3% to 66.4%. For a fixed ratio of renewable generation capacity and grid capacity, renewable generation curtailment is minimized.

Optimal battery capacities are largely uncorrelated with the total renewable and grid capacities. Additional perspective is shown in Fig. 9 by plotting the wind and solar capacities on separate axis. As in the 2023 case, the optimal battery capacity for the system is impacted by the ratio between the installed wind and solar capacities with larger battery capacities being needed for system designs with a high fraction of solar generation.

While moving to net zero carbon emissions in 2050 may still increase the microgrid LCOE as compared to the optimal 2023 case, it increases by far less than when done without development of local energy generation and remains far less than the business as usual 2050 LCOE. This indicates that building local generation resources at the grid edge in the right conditions can improve microgrid economics in addition to improving the system reliability and reducing reliance on the national electric grid. Application of the novel multiscale optimization technique to this problem provides insight into the tradeoffs between technical feasibility and economic outcomes for a range of relevant values near the exact optimum.

5. Conclusions

The capacities of a grid-connected HES is optimized using a unique multiscale method as well as a direct solution, providing insight into the technoeconomic tradeoffs associated with near-optimal unit capacities. This is done for both approximate 2023 grid conditions and forecasted 2050 conditions with net zero carbon emissions for a total CO_2 reduction of 19920 tones/yr. The results are also compared to the local economics

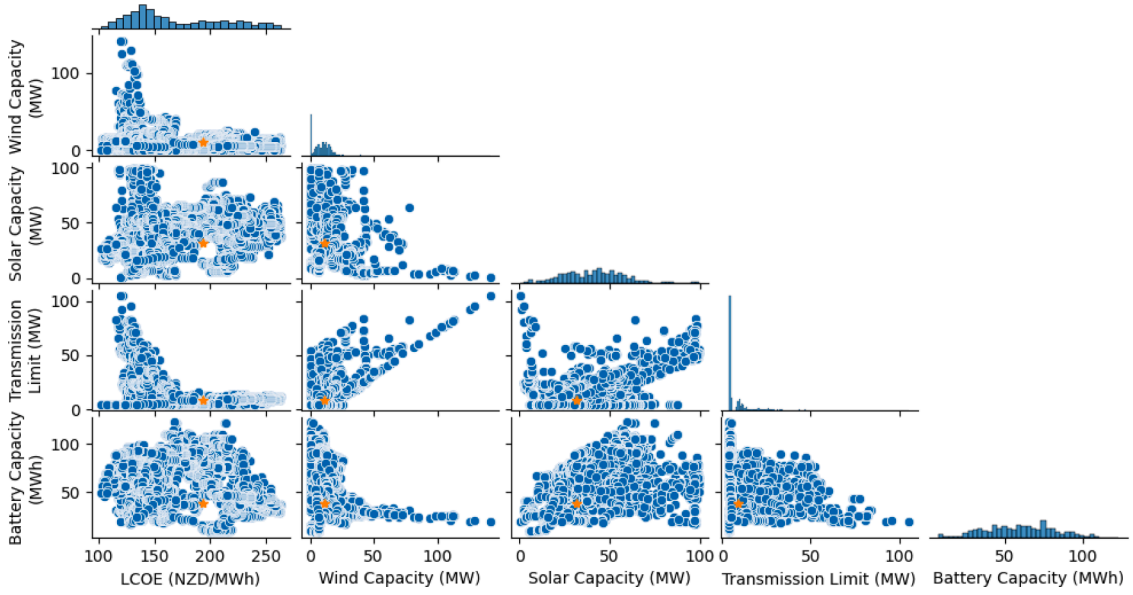

Fig. 7. The optimal capacity distribution for the 2050 net zero case. Gold stars indicate the exact solution to the problem.

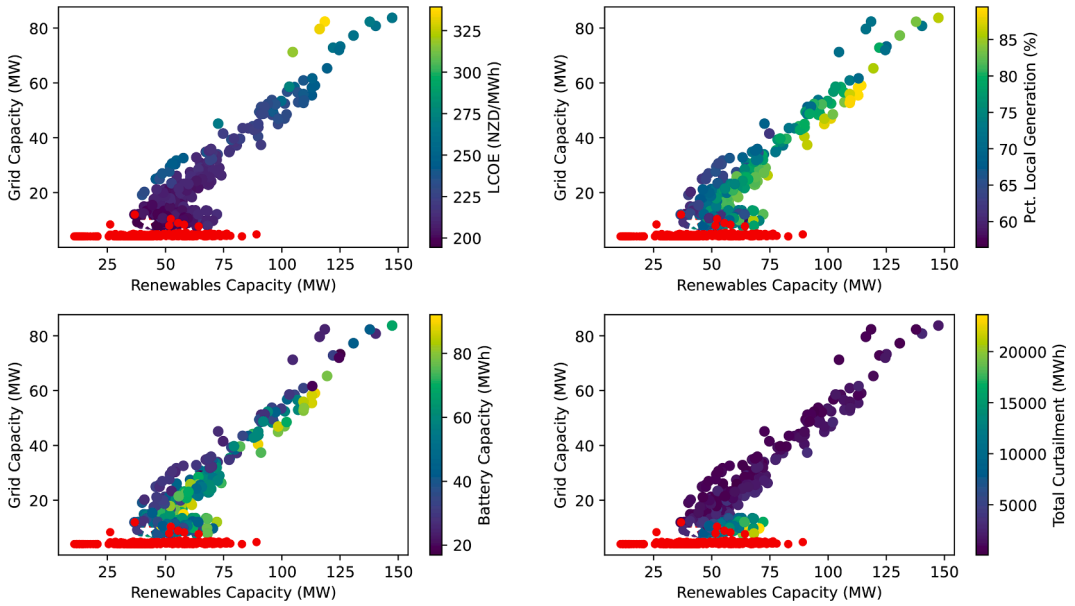

Fig. 8. Metrics results for the 2050 curtailed case. White stars represent the metrics at the exact solution to the problem. Red dots indicate examined capacities that cannot satisfy demand for the whole year.

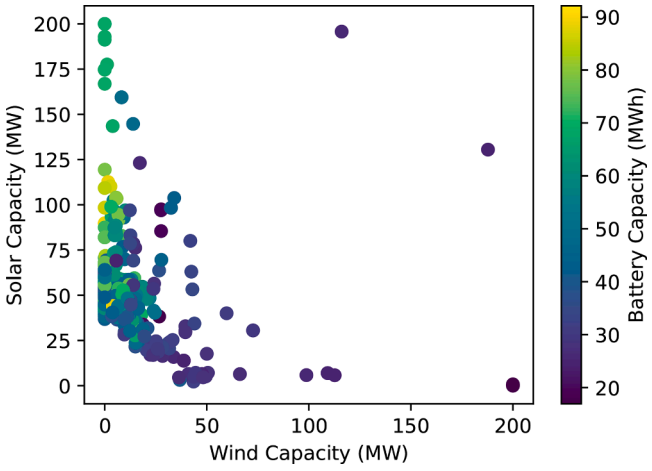

Fig. 9. Optimal battery capacities as a function of installed wind and solar capacities for net zero 2050.

if no local generation is developed. The technoeconomic impacts of limited-capacity grid transmission line upgrades are included providing relevant insight and techniques for optimizing local generation and storage versus grid dependence. Local generation and hybridization allows for a 36.8% reduction of LCOE in the 2023 case and a 38.6% reduction in the 2050 case. Building grid-edge HES can reduce grid interconnection requirements, potentially improving system economics while decreasing overall carbon emissions.

Allowing curtailment in grid-connected HES increases the optimal percentage of electricity generated locally 4.8% for 2023 and 2.1% for 2050, decreasing reliance on the larger power grid. Allowing curtailment also results in a decrease of the optimal LCOE by 4 NZD/MWh for both cases. Overall curtailment of renewable energy generation is determined to be a key consideration and is shown to improve performance of grid-connected HES in both economics and robustness.

Finally additional development of a novel multiscale optimization algorithm for HES is presented and validated on the sample problems in this work. This algorithm provides additional context and perspective into the optimal capacity sizing problem allowing identification of optimal designs that may not be robust to future conditions.

Future work

There are multiple limitations of this work which can broadly be broken down into modeling limitations and algorithmic limitations. The model limitations include simplifications that could impact the accuracy of the work. Predicted changes to grid electricity prices between 2023 and 2050 are not considered. As New Zealand moves towards net zero carbon emissions, both the average cost of electricity and the price dynamics are highly likely to change. No reliable estimations of future grid pricing were available and modeling the technoeconomics of the larger grid to produce reasonable estimates is outside this scope of work. Similarly, the impact of microgrid connection on the price of electricity across the larger grid is also not considered. Electrification of heavy trucking and the potential development of a hydrogen ecosystem are also neglected. This work also does not consider the impact of geographically-distributed generation across New Zealand. While this work focuses on local generation in order to reduce grid transmission requirements, some areas will not be restricted in this way and may benefit more from distributed generation.

Multiple optimization algorithm limitations also exist. While the current implementation is capable of handling complex models over long time horizons the algorithm does not scale efficiently to larger problem sizes. In the first stage of the algorithm as described in Section 2.3, all possible subsets of length τ are used in computing the multi-dimensional distribution of optimal capacities. Using a representative sample rather than all possible subsets would vastly improve the computational performance of the algorithm, but it remains to be determined how a representative sample could be determined efficiently. Similarly, the minimum required number of samples used in the second stage is not well known, resulting in oversampling. Reducing the number of samples required for proper characterization of the output space would also greatly improve algorithm scalability.

CRediT authorship contribution statement

Daniel Hill: Conceptualization, Data curation, Formal analysis, Investigation, Methodology, Software, Visualization, Writing – original draft, Writing – review & editing. **Shafiqur Rahman Tito:**

Conceptualization, Investigation, Project administration, Resources, Supervision, Writing – review & editing. **Michael Walmsley:** Conceptualization, Formal analysis, Funding acquisition, Project administration, Supervision, Writing – original draft, Writing – review & editing. **John Hedengren:** Conceptualization, Formal analysis, Funding acquisition, Project administration, Supervision, Writing – original draft, Writing – review & editing.

Declaration of competing interest

The authors declare that they have no known competing financial interests or personal relationships that could have appeared to influence the work reported in this paper.

Data availability

The authors do not have permission to share data.New Zealand Grid Optimization

Acknowledgements

The authors gratefully acknowledge funding from the United States Department of Energy [DE-NE0008866] and assistance from researchers at Idaho National Laboratory. The authors also gratefully acknowledge support and assistance from the Ahuora Centre for Smart Energy Systems.

Supplementary material

Supplementary material associated with this article can be found, in the online version, at 10.1016/j.prime.2024.100564.

References

[1] Ministry for the Environment, Climate change response (zero carbon) amendment act 2019, 2021. https://environment.govt.nz/acts-and-regulations/acts/climate-change-response-amendment-act-2019/, Last accessed on 23 Jun 2023.
[2] T.T.P. Bui, S. Wilkinson, N. Domingo, C. MacGregor, Zero carbon building practices in Aotearoa New Zealand, Energies 14 (15) (2021), https://doi.org/10.3390/en14154455.
[3] F. Reguyal, K. Wang, A.K. Sarmah, Electrification of New Zealand transport: environmental impacts and role of renewable energy, Sci. Total Environ. 894 (2023) 164936, https://doi.org/10.1016/j.scitotenv.2023.164936.
[4] S.P. Yue Wang Basil Sharp, K.-M. Nam, Economic and land use impacts of net zero-emission target in New Zealand, Int. J. Urban Sci. 26 (2) (2022) 291–308, https://doi.org/10.1080/12265934.2020.1869582.
[5] M.R. Walmsley, T.G. Walmsley, M.J. Atkins, P.J. Kamp, J.R. Neale, Minimising carbon emissions and energy expended for electricity generation in New Zealand through to 2050, Appl. Energy 135 (2014) 656–665, https://doi.org/10.1016/j.apenergy.2014.04.048.
[6] T. Stevenson, S. Batstone, D. Reeve, M. Poynton, C. Comendant, Transitioning to Zero Net Emissions by 2050: Moving to a Very Low-Emissions Electricity System in New Zealand. Technical Report, SAPERE Research Group, 2018.
[7] M. Wei, C.A. McMillan, S. de la Rue du Can, Electrification of industry: potential, challenges and outlook, Curr. Sustain./Renew. Energy Rep. 6 (2019) 140–148, https://doi.org/10.1007/s40518-019-00136-1.
[8] A. Grenier, S. Page, The impact of electrified transport on local grid infrastructure: a comparison between electric cars and light rail, Energy Policy 49 (2012) 355–364, https://doi.org/10.1016/j.enpol.2012.06.033.Special Section: Fuel Poverty Comes of Age: Commemorating 21 Years of Research and Policy
[9] R. Strahan, A. Miller, Q. Tahau, Systems to implement demand response in New Zealand, Electricity Engineers' Association Conference, Auckland, New Zealand, 2014.https://hdl.handle.net/10092/100664
[10] N. Majdi Nasab, J. Kilby, L. Bakhtiaryfard, Case study of a hybrid wind and tidal turbines system with a microgrid for power supply to a remote off-grid community in New Zealand, Energies 14 (12) (2021), https://doi.org/10.3390/en14123636.
[11] A.H. Fathima, K. Palanisamy, Optimization in microgrids with hybrid energy systems – a review, Renew. Sustain. Energy Rev. 45 (2015) 431–446, https://doi.org/10.1016/j.rser.2015.01.059.
[12] O. Olabode, T. Ajewole, I. Okakwu, A. Alayande, D. Akinyele, Hybrid power systems for off-grid locations: a comprehensive review of design technologies, applications and future trends, Sci. Afr. 13 (2021) e00884, https://doi.org/10.1016/j.sciaf.2021.e00884.
[13] B. Zhao, M. Cheng, C. Liu, Z. Dai, Conceptual design and preliminary performance analysis of a hybrid nuclear-solar power system with molten-salt packed-bed thermal energy storage for on-demand power supply, Energy Convers. Manage. 166 (2018) 174–186.https://www.sciencedirect.com/science/article/pii/S0196890418303509
[14] A. Ho, K. Mohammadi, M. Memmott, J. Hedengren, K.M. Powell, Dynamic simulation of a novel nuclear hybrid energy system with large-scale hydrogen storage, Int. J. Hydrogen Energy 46 (2021) 31143–31157, https://doi.org/10.1016/j.ijhydene.2021.07.027.
[15] Transpower, Transmission Lines - Transline, 2023, (https://services3.arcgis.com/AkUq3zcWf7TVqyR9/arcgis/rest/services/TransmissionLines/FeatureServer/0). Accessed: 26 Jul 2023.
[16] M. Apperley, T. Toki, An islanded community solar microgrid with capability of future fractal growth. ENERGY 2023 Proceedings, 2023, p. 35.
[17] M. Apperley, P. Monigatti, J. Suppers, Grid-lite: a network integrated semi-autonomous local area electricity system. Proceedings of the 4th International Conference on Green IT Solutions, 2015, pp. 27–33.
[18] P.W. Talbot, A. Gairola, P. Prateek, A. Alfonsi, C. Rabiti, R.D. Boardman, HERON as a Tool for LWR Market Interaction in a Deregulated Market. Technical Report, Idaho National Lab, 2019, https://doi.org/10.2172/1581179.
[19] K.H. Anderson, D.S. Cutler, D.R. Olis, E.M. Elgqvist, X. Li, N.D. Laws, N.A. DiOrio, H.A. Walker, REopt: A Platform for Energy System Integration and Optimization. Technical Report, National Renewable Energy Lab, 2017, https://doi.org/10.2172/1395453.
[20] R.D. López, iHOGA/MHOGA, 2022, (https://ihoga.unizar.es/en/). Accessed: 1 Dec 2022.
[21] U.H. Software, Homer grid 1.8, 2022, (https://www.homerenergy.com/products/grid/docs/1.8/optimization_settings.html). Accessed: 1 Dec 2022.
[22] S. Sinha, S. Chandel, Review of software tools for hybrid renewable energy systems, Renew. Sustainable Energy Reviews 32 (2014) 192–205.
[23] A.S. Tukkee, N.I. bin Abdul Wahab, N.F. binti Mailah, Optimal sizing of autonomous hybrid microgrids with economic analysis using grey wolf optimizer technique, e-Prime - Adv. Electr. Eng. Electron. Energy 3 (2023) 100123, https://doi.org/10.1016/j.prime.2023.100123.
[24] D. Hill, D. McCrea, A. Ho, M. Memmott, K. Powell, J. Hedengren, A multi-scale method for combined design and dispatch optimization of nuclear hybrid energy systems including storage, e-Prime - Adv. Electr. Eng. Electron. Energy 5 (2023) 100201, https://doi.org/10.1016/j.prime.2023.100201.
[25] W. Chen, M. Fuge, Active expansion sampling for learning feasible domains in an unbounded input space, Struct. Multidiscip. Optim. 57 (2018) 925–945.
[26] H. Ritchie, M. Roser, P. Rosado, CO_2 and greenhouse gas emissions, Our World in Data (2022).Https://ourworldindata.org/co2-and-greenhouse-gas-emissions
[27] S.N. Zealand, 2013 QuickStats about families and households. Technical Report, stats.govt.nz, 2014.
[28] NZ.Stat, National population projections, characteristics, 2022(base)-2073, 2022, https://nzdotstat.stats.govt.nz/wbos/Index.aspx.
[29] E. Klinac, J.K. Carson, D. Hoang, Q. Chen, D.J. Cleland, T.G. Walmsley, Multi-level process integration of heat pumps in meat processing, Energies 16 (8) (2023), https://doi.org/10.3390/en16083424.
[30] M.T. Bahr, J. Immonen, B.W. Billings, K.M. Powell, Intelligent control of thermal energy storage in the manufacturing sector for plant-level grid response, Processes 11 (7) (2023), https://doi.org/10.3390/pr11072202.
[31] P.S.C.N.Z. Limited, Ripple Control of Hot Water in New Zealand. Technical Report, Energy Efficiency and Conservation Authority, Wellington, New Zealand, 2020.
[32] P. Paevere, A. Higgins, Z. Ren, M. Horn, G. Grozev, C. McNamara, Spatio-temporal modelling of electric vehicle charging demand and impacts on peak household electrical load, Sustain. Sci. 9 (2014) 61–76, https://doi.org/10.1007/s11625-013-0235-3.
[33] C. Rodgers, A. Siddique, J. Ferreira, T. Johnson, ElectraNet Transmission Line Cost Review. Technical Report, Jacobs Group Pty Limited, 2019.https://www.electranet.com.au/wp-content/uploads/projects/2016/11/ElectraNet-Transmission-Line-Cost-Review-Jacobs.pdf
[34] L.D.R. Beal, D.C. Hill, R.A. Martin, J.D. Hedengren, GEKKO optimization suite, Processes 6 (8) (2018), https://doi.org/10.3390/pr6080106.
[35] A. Wächter, L.T. Biegler, On the implementation of an interior-point filter line-search algorithm for large-scale nonlinear programming, Math. Program. 106 (1) (2006) 25–57, https://doi.org/10.1007/s10107-004-0559-y.
[36] NIWA, Solarview, 2019, https://niwa.co.nz/our-services/online-services/solarview, Last Accessed on 26 Jun 2023.
[37] S. Tito, T. Lie, T. Anderson, Optimal sizing of a wind-photovoltaic-battery hybrid renewable energy system considering socio-demographic factors, Solar Energy 136 (2016) 525–532, https://doi.org/10.1016/j.solener.2016.07.036.
[38] M.R.W. Walmsley, E. Klinac, S. Tito, M.J. Atkins, M. Apperley, Integration of localised renewable energy into a meat processing site. Proceedings of the 26th Conference on Process Integration, Modeling and Optimisation for Energy Saving and Pollution Reduction, PRES23, Thessaloniki, Greece, 2023.
[39] S. Quotes, Solar power buy-back rates, https://www.mysolarquotes.co.nz/about-solar-power/residential/solar-power-buy-back-rates-nz/.
[40] G.R. Timilsina, Are renewable energy technologies cost competitive for electricity generation? Renew. Energy 180 (2021) 658–672, https://doi.org/10.1016/j.renene.2021.08.088.
[41] W. Cole, A.W. Frazier, C. Augustine, Cost Projections for Utility-Scale Battery-Storage: 2021 Update. Technical Report, National Renewable Energy Laboratory, 2021, https://doi.org/10.2172/1786976.

[42] IEA, World Energy Outlook 2020. Technical Report, IEA, 2020.https://www.iea.org/reports/world-energy-outlook-2020
[43] A. Miller, Economics of Utility-Scale Solar in Aotearoa New Zealand. Technical Report, Allan Miller Consulting Ltd., 2020.
[44] D. Hill, A. Martin, N. Martin-Nelson, C. Granger, M. Memmott, K. Powell, J. Hedengren, Techno-economic sensitivity analysis for combined design and operation of a small modular reactor hybrid energy system, Int. J. Thermofluids 16 (2022) 100191, https://doi.org/10.1016/j.ijft.2022.100191.

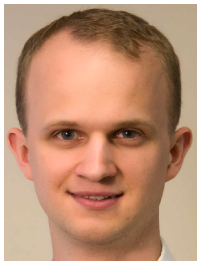

Daniel Hill is a PhD Candidate at Brigham Young University focused on combined design and dispatch optimization for nuclear-renewable hybrid energy systems. He is a member of the Schneider Electric advanced process control group with development responsibilities for system identification, optimization, and optimal control of multivariate systems. His prior experience includes research assistant for the DIPPR Thermophysical Properties Lab and his 8 publications have been cited 313 times.

Dr. Shafiqur Rahman Tito received his PhD degree in electrical engineering from the Auckland University of Technology (AUT), Auckland, New Zealand, in 2016. He completed his MSc and BSc degree from the University of Ulm, Ulm, Germany and Islamic Institute of Technology (IIT) [Currently known as Islamic University of Technology]. He was supported with a Engineering Doctoral Scholarship for his PhD and OIC scholarship (3 out of 4 years) for his BSc. His employment experience includes 12 years of teaching at different international Institute - IUT(Bangladesh), IIUM (Malaysia) AUT (New Zealand) and Waikato University (New Zealand). He had been working as a senior lecturer in electrical engineering Department of Manukau Institute of Technology, Auckland before joining to Ahuora - Centre for Smart Energy Systems: University of Waikato as a postdoctoral research fellow. His current research interest includes hybrid renewable energy systems (HRES), optimization, smart grid, microgrid, energy efficiency, load disaggregation, smart energy management system and internet of things (IoT).

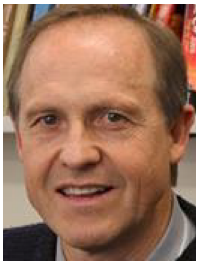

Professor Michael Walmsley has extensive curriculum, teaching and research experience from a 36 year academic career in Chemical and Process Engineering. He leads the Ahuora Centre for Smart Energy Systems at the University of Waikato, where energy digital twin technology combined with open-source process integration and energy system analysis tools are being developed to help NZ industry fully decarbonize, through improved energy efficiency, adoption of high temperature heat pumps and cost effective integration of renewable energy into their operations.

Dr. John Hedengren is a Professor at Brigham Young University in the Chemical Engineering Department. He leads the BYU Process Research and Intelligent Systems Modeling (PRISM) group with a focus on structured machine learning for optimization of energy systems, unmanned aircraft, and drilling. Prior to BYU he worked in industry for 7 years on nonlinear estimation and predictive control for polymers. His work includes the APMonitor Optimization Suite with a recent extension to the Python GEKKO language. He led the development of the Arduino-based Temperature Control Lab that is currently used by 70 universities for process control education. His 85 publications span topics of data science, machine learning, smart grid optimization, unmanned aerial systems, and predictive control.